Abdominal Radiology

Published online: 7 June 2016

Abdom Radiol (2016) 41:1937–1941
DOI: 10.1007/s00261-016-0791-y

Value of diffusion-weighted MR imaging in the diagnosis of lymph node metastases in patients with cholangiocarcinoma

Konstantin Holzapfel,[1] Jochen Gaa,[1] Elaine C. Schubert,[1] Matthias Eiber,[2] Joerg Kleeff,[3] Ernst J. Rummeny,[1] Martin Loos[3]

[1]Department of Radiology, Klinikum rechts der Isar der Technischen Universität München, Ismaninger Str. 22, 81675 Munich, Germany
[2]Department of Nuclear Medicine, Klinikum rechts der Isar der Technischen Universität München, Ismaninger Str. 22, 81675 Munich, Germany
[3]Department of Surgery, Klinikum rechts der Isar der Technischen Universität München, Ismaninger Str. 22, 81675 Munich, Germany

Abstract

Purpose: To evaluate diffusion-weighted MR imaging (DWI) in the diagnosis of lymph node metastases in patients with cholangiocarcinoma.
Methods: In 24 patients with cholangiocarcinoma, MR imaging of the upper abdomen was performed prior to surgery at 1.5 T using a respiratory-triggered single-shot echo-planar imaging (SSEPI) sequence (*b* values: 50, 300, and 600 s/mm^2). ADC (apparent diffusion coefficient) values and diameters of regional lymph nodes (LN) were determined. Subsequently, in all patients, surgical exploration and/or resection of the primary tumor and regional LN dissection were performed. Imaging results were correlated with results of histopathologic analysis. ADC values and diameters of benign and malignant LN were compared using the Mann–Whitney *U* test. In addition, a ROC (receiver operating characteristic curve) analysis was performed.
Results: The mean ADC value ($\times 10^{-3}$ mm^2/s) of metastatic LN (1.21 ± 0.15) was significantly lower than that of benign LN (1.62 ± 0.33, $p < 0.001$) while there was no significant difference in the mean diameter of malignant (16.8 ± 5.4 mm) and benign LN (14.1 ± 4.0 mm; $p = 0.09$). Using an ADC value of 1.25×10^{-3} mm^2/s as threshold, 91.4% of LN were correctly classified as benign or malignant with a sensitivity/specificity of 83.3%/92.8% and a positive/negative predictive value of 66.7%/96.7%. The area under the ROC curve was 0.93.
Conclusion: DWI using a respiratory-triggered SSEPI sequence, according to our preliminary experience, is a promising imaging modality in the differentiation of benign and malignant LN in patients with cholangiocarcinoma.

Key words: Cholangiocarcinoma—Lymph node metastases—MR imaging—Diffusion-weighted MR imaging (DWI)

Cholangiocarcinoma, i.e., carcinoma arising from the ductal epithelium of the intrahepatic, perihilar, and extrahepatic bile ducts is rare and its prognosis is very poor [1]. The only curative treatment is complete resection with negative surgical margins [1–5]. Preoperative evaluation of the tumor is important in order to evaluate resectability and the extent of surgery. This entails not only determination of the exact boarders of the primary tumor (T-staging) but also the detection of regional lymph node metastases. The regional lymph nodes (LN) include hilar, celiac, periduodenal, peripancreatic, and superior mesenteric LN [6]. Usually, the criteria for identification of metastatic LN on cross-sectional imaging are as follows: larger than 10 mm in short-axis diameter, presence of central necrosis, and hyperattenuation compared to the liver in the portal venous phase if CT imaging is used [7]. However, reported sensitivities and specificities of CT, MR imaging, and FDG-PET in

Correspondence to: Konstantin Holzapfel; *email:* holzapfel@roe.med.tum.de

the nodal staging of cholangiocarcinoma are moderate, and false-negative cases are frequently encountered [8–10]. In addition, false-positives can be seen, e.g., in patients with primary sclerosing cholangitis (PSC) where reactively enlarged LN are a common finding. Therefore, lymph node status cannot be reliably determined on the current imaging system, and the presence of equivocal LN cannot be used as a criterion for unresectability. Some surgeons prefer paraaortic lymph node sampling before proceeding to an intended curative resection [11, 12], and staging operation with LN sampling has been suggested for unresectable cholangiocarcinoma prior to liver transplantation [13].

Diffusion-weighted imaging (DWI) is a form of MR imaging based on measuring the random Brownian motion of water molecules within a voxel of tissue. In recent years, DWI has been increasingly used for tumor detection and characterization throughout the body [14]. In addition, there is an emerging role of DWI as a potential MR biomarker [14]. Low apparent diffusion coefficient (ADC) values seen in malignant tumors and LN metastases probably reflect distinct histopathologic features. In general, malignant tissues tend to be hypercellular, nuclei are enlarged, hyperchromatic with abundant macromolecular proteins [15]. In addition, the extracellular space is small [15]. These factors reduce the diffusion space for water protons in the intra- and extracellular compartment resulting in a decrease of ADC values. In contrast to metastatic nodes, benign LN show lower cellularity, smaller nuclei, lower nucleus-to-cytoplasma ratios, and more extracellular space, a tissue architecture considered to allow better water diffusibility and resulting in high ADC values compared to malignant tissue [15, 16]. Regarding the diagnosis of LN metastases, a potential role of DWI has been studied for a number of tumors and regions of the body [17, 18]. In addition, DWI has been evaluated in the diagnosis of the primary tumor in patients with cholangiocarcinoma [19, 20], however, to the best of our knowledge not in the diagnosis of LN metastases in these patients. Hence, the purpose of our study was to evaluate DWI in the diagnosis of LN metastases in patients with cholangiocarcinoma.

Materials and methods

Patients

The study was approved by our institutional review board. As images were analyzed retrospectively in this single-center study, the requirement for informed consent was waived. A query of our image database revealed a total of 78 patients with newly diagnosed cholangiocarcinoma who had undergone MR imaging between January 2007 and June 2013. In 34 of those patients, surgical exploration and/or resection of the tumor including regional LN dissection was performed. Only patients with standardized MR examination performed at our institution including DWI of the upper abdomen were included in the study. Therefore, the final study population consisted of 24 patients (14 men, 10 women, mean age 65.4 ± 9.7 years, age range 41–83 years). Among those, there were four patients with PSC.

Standard of reference

All patients underwent surgery and local LN dissection was performed. Therefore, histopathologic confirmation was available in all patients. A mean of 10.4 ± 7.9 LN was resected in each patient (range 2–30). Intraoperatively, the localization of resected LN was documented in order to allow correlation of imaging findings and results of surgery and histopathologic analysis. In order to correctly assign LN seen in DWI with intraoperative findings and results of histopathologic analysis and to optimize radiologic–pathologic correlation, a stepwise approach was applied. Preoperatively, MR images were analyzed by radiologist and surgeon in consensus. Intraoperatively, hilar, celiac, periduodenal, peripancreatic, and superior mesenteric LN were assessed/resected. Anatomic localization of resected LN was accurately documented during surgery. Postoperatively, intraoperative and pathologic findings were again correlated with findings at MR imaging in consensus. In cases of clustering of LN within the same anatomic region, the largest LN were analyzed. LN diameters determined by pathologic analysis and MR imaging were used as a marker for the radiologic–pathologic correlation.

MR imaging

MR imaging was performed on a 1.5-T system (Magnetom Avanto, Siemens Medical Solutions, Erlangen, Germany) with two six-channel body phased array coils anterior and two spine clusters (three channels each) posterior. In addition to DWI (see below), at least a coronal T2-weighted half-Fourier single-shot turbo spin-echo (HASTE) sequence and an axial T2-weighted turbo spin-echo sequence were acquired as well as an axial dynamic T1-weighted, three-dimensional spoiled gradient-recalled echo sequence (volumetric interpolated breath-hold examination (VIBE) sequence with spectral fat saturation) following the intravenous administration of Gd-DTPA.

Diffusion-weighted images were acquired using a single-shot echo-planar imaging sequence. In order to acquire images with a high contrast-to-noise ratio for optimal conspicuity of LN while keeping the influence of ''pseudodiffusion'' by means of perfusion effects low, the minimum gradient factor (b value) was set at 50 s/mm^2. Thus, the gradient factors (b values) were 50, 300, and 600 s/mm^2. The technical parameters were as follows: echo time, 69 ms; echo train length, 58; echo spacing,

0.69 ms; receiver bandwidth, 1736 Hz/pixel; spectral fat saturation; field of view, 263 × 350 mm; matrix, 144 × 192; section thickness, 5 mm. For shortening of the echo train length, integrated parallel imaging techniques (iPAT) by means of generalized autocalibrating partially parallel acquisitions (GRAPPA) with a twofold acceleration factor were used. For respiratory triggering, PACE (prospective acquisition correction) was implemented. Data were acquired during the end-expiratory phase. DWI was performed before the administration of Gd-DTPA.

Image analysis

Review of all MR images was performed on a commercial PACS workstation (Easy vision, Philips, Best, The Netherlands). Images acquired using DWI were evaluated by a radiologist with 10 years' experience who was specialized in abdominal MR imaging. Images were analyzed in random order. The reader was free to alter window level and window width at his discretion. Except for knowing that patients had been examined for known or suspected cholangiocarcinoma, the reader was blinded to MR imaging reports, findings of other MR sequences, clinical history, and pathologic results. The reader documented presence and location of local LN. The reader localized LN as hilar, celiac, periduodenal, peripancreatic, and superior mesenteric and was free to add any additional information in order to be as precise as possible. The maximum diameter of each LN in the short axis was measured. Diameter of LN was used as an additional tool to optimize radiologic–pathologic correlation. Only LN with a diameter of 8 mm and more were included in the analysis. In addition, measurement of ADC values was performed using DWI. A circular region of interest (ROI) encompassing as much of LN as possible was drawn on the low b value (b = 50 s/mm^2) image (where LN show the highest conspicuity) and transferred to the ADC map. Areas of marked signal hyperintensity on T2-weighted images, suggestive of necrosis, were excluded from the analysis.

Statistical analysis

Statistical analysis was performed using SPSS (version 16.0, SPSS Inc., Chicago, IL. USA) and Graph-Pad Prism 4 software package for Windows. Imaging results were correlated with results of histopathologic analysis. ADC values and diameters of benign and malignant LN were compared using the Mann–Whitney U test. In addition, a ROC (receiver operating characteristic curve) analysis was performed to determine the diagnostic capability of ADC values in the differentiation of benign from malignant LN and to determine the threshold of ADC values providing the highest accuracy for discriminating benign from malignant LN. Bonferroni correction was used for multiple pairwise comparisons.

Results

A total of 70 LN were analyzed by DWI. In none of these, LN necrosis was observed in MR imaging. Of the 70 LN, 13 LN in eight of the 24 patients were metastases, 57 LN were benign in pathology. In histopathologic analysis, a total of 201 LN were reported. Of those 131 were not visible in DWI or too small for analysis (diameter <8 mm). LN metastases were reported in nine of the patients. Of those, one patient had LN metastases that were not seen in DWI (diameter of ≤3 mm in histopathology). The mean diameter of benign LN that were analyzed by DWI was 14.1 ± 4.0 mm compared to 16.8 ± 5.4 mm of malignant LN. There was no statistically significant difference in the mean diameter of benign and malignant LN (p = 0.09) (Fig. 1). The mean diameter of LN in patients with PSC was 14.5 ± 3.5 mm and was not significantly different from the mean diameter of malignant LN (p = 0.18). On diffusion-weighted MR images, metastatic nodes showed high signal intensities at b values of 50, 300, and 600 s/mm^2 and, consequently, low signal intensities on ADC maps (Fig. 2). In contrast, most reactively enlarged benign lymph nodes showed high signal intensities at b = 50 s/mm^2, comparatively low signal intensities at b = 600 s/mm^2 and were bright on ADC maps (Fig. 3). The mean ADC value ($\times 10^{-3}$ mm^2/s) of metastatic LN (1.21 ± 0.15) was significantly lower than that of benign LN (1.62 ± 0.33, $p < 0.001$) (Fig. 4). The optimal threshold ADC value for differentiating between benign and malignant LN determined by ROC analysis was 1.25 × 10^{-3} mm^2/s. Applying this value, 91.4% of LN were correctly classified as benign or malignant with a sensitivity/specificity of 83.3%/92.8% and a positive/negative predictive value of 66.7%/96.7%. The area under the ROC curve was 0.93 (Fig. 5).

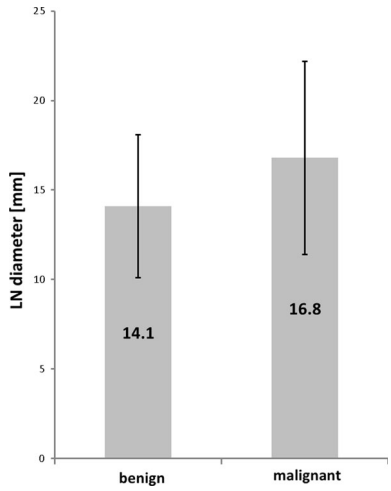

Fig. 1. Mean diameter of benign and malignant LN. There is no statistically significant difference in the mean diameter of benign and malignant LN (p = 0.09).

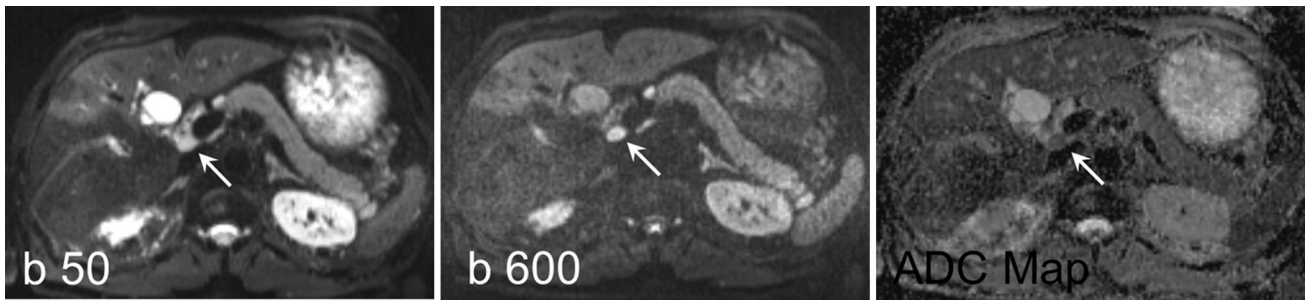

Fig. 2. A moderately enlarged LN adjacent to the portal vein (*arrow*) is hyperintense at a low and a high b value and shows a low ADC value (0.98×10^{-3} mm^2/s). Histopathologic analysis revealed a LN metastasis.

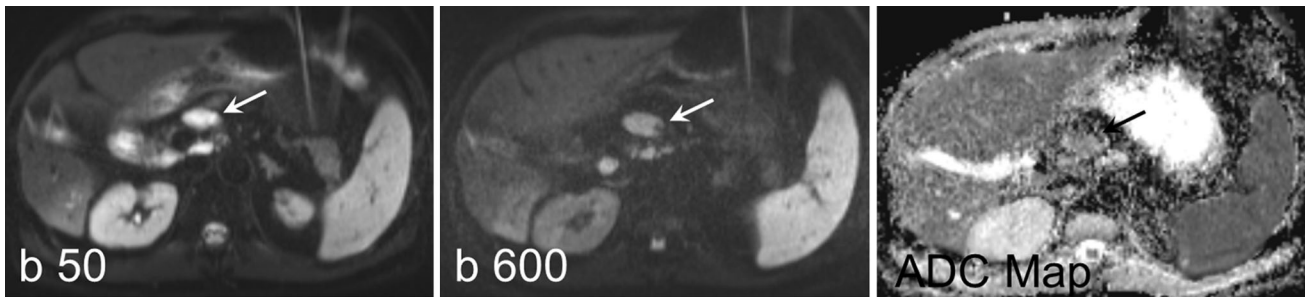

Fig. 3. An enlarged LN adjacent to the portal vein (*arrow*) is hyperintense at a low *b* value, shows some signal loss at a higher *b* value and has a high ADC value (1.46×10^{-3} mm^2/s). In this case, no malignant LN were found in histopathologic analysis.

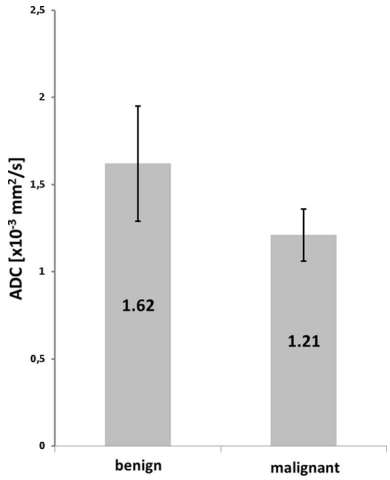

Fig. 4. Mean ADC values of benign and malignant LN. The mean ADC value of metastatic LN was significantly lower than that of benign LN ($p < 0.001$).

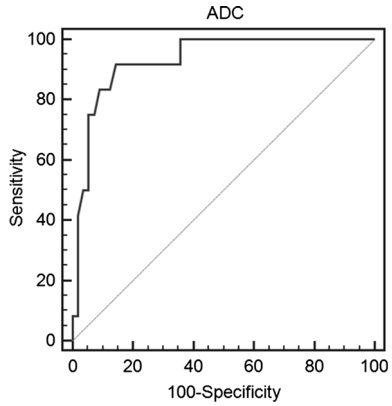

Fig. 5. ROC curve for differentiating benign from metastatic LN using ADC values. The area under the ROC curve was 0.93.

Discussion

In our study, we demonstrated that in patients with cholangiocarcinoma, ADC values of regional LN metastases are significantly lower than those of benign LN and thus, DWI seems to have the potential to elucidate the differentiation between benign and malignant LN.

Correct characterization of LN is crucial for staging, therapy planning, and follow-up of patients with cholangiocarcinoma. Although detection of enlarged LN is possible by modern cross-sectional imaging modalities, the differentiation between benign and malignant LN remains challenging as none of the morphological criteria, including size, shape, or presence of necrosis is absolutely reliable.

Despite a statistically significant difference, considerable overlap of ADC values of benign and malignant

LN was observed in the present study (Fig. 4) and the accuracy of diagnosing or excluding LN metastases is <100%. However, the high negative predictive value (96.7%) observed in the present study may serve as a helpful indicator in the decision pro or against surgery. Other studies have shown an overlap in ADC values of the primary tumor in patients with intrahepatic and hilar mass-forming cholangiocarcinoma [20]. Hence, an overlap of ADC values of LN metastases is not surprising.

Our study has some limitations. Firstly, although the vendor supplied sequence was improved at our institution, susceptibility artifacts and image distortions along the phase encoding gradient could not be eliminated completely. Thus, only LN measuring 8 mm and more were analyzed. Determination of accurate ADC values in smaller lymph nodes currently seems to be unreliable. Particularly, measuring ADC values adjacent to air-containing organs remains challenging because of susceptibility artifacts. Furthermore, we want to stress that the optimal threshold ADC value for differentiating benign from malignant LN has to be determined for each MR imaging system, as there are variations in MR units and pulse sequences. Finally, the number of patients included in our study was limited. In particular, the number of patients with PSC was very small.

DWI using a single-shot echo-planar imaging sequence is a promising tool for the differentiation of benign and malignant LN in patients with cholangiocarcinoma. As signal properties on DWI reflect the microstructure and the physiologic state of tissue independent from LN size, in the future it may be possible to characterize even small LN as benign or malignant. However, further technical advances are necessary to improve spatial resolution and to reduce susceptibility and motion artifacts in DWI.

Compliance with ethical standards

Conflict of interest There is no conflict of interest.

Ethical approval All procedures performed in studies involving human participants were in accordance with the ethical standards of the institutional and/or national research committee and with the 1964 Helsinki declaration and its later amendments or comparable ethical standards. The study was approved by our institutional review board. As images were analyzed retrospectively in this single-center study, the requirement for informed consent was waived.

References

1. Khan SA, Thomas HC, Davidson BR, Taylor-Robinson SD (2005) Cholangiocarcinoma. Lancet 366:1303–1314
2. Lazaridis KN, Gores GJ (2005) Cholangiocarcinoma. Gastroenterology 128:1655–1667
3. Patel T (2006) Cholangiocarcinoma. Nat Clin Pract Gastroenterol Hepatol 3:33–42
4. Bold RJ, Goodnight JE Jr (2004) Hilar cholangiocarcinoma: surgical and endoscopic approaches. Surg Clin North Am 84:525–542
5. De Groen PC, Gores GJ, LaRusso NF, Gunderson LL, Nagorney DM (1999) Biliary tract cancers. N Engl J Med 341:1368–1378
6. Green FL, Page DL, Fleming ID, et al. (2002) *AJCC cancer staging manual*. New York: Springer
7. Lee HY, Kim SH, Lee JM, et al. (2006) Preoperative assessment of resectability of hepatic hilar cholangiocarcinoma: combined CT and cholangiography with revised criteria. Radiology 239:113–121
8. Roche CJ, Hughes ML, Garvey CJ, et al. (2003) CT and pathologic assessment of prospective nodal staging in patients with ductal adenocarcinoma of the head of the pancreas. AJR Am J Roentgenol 180:475–480
9. Kluge R, Schmidt F, Caca K, et al. (2001) Positron emission tomography with [(18)F]fluoro-2-deoxy-D-glucose for diagnosis and staging of bile duct cancer. Hepatology 33:1029–1035
10. Hanninen EL, Pech M, Jonas S, et al. (2005) Magnetic resonance imaging including magnetic resonance cholangiopancreatography for tumor localization and therapy planning in malignant hilar obstructions. Acta Radiol 46:462–470
11. Yoshida T, Matsumoto T, Sasaki A, et al. (2004) Outcome of paraaortic nodepositive pancreatic head and bile duct adenocarcinoma. Am J Surg 187:736–740
12. Shimada K, Sakamoto Y, Sano T, Kosuge T (2006) The role of paraaortic lymph node involvement on early recurrence and survival after macroscopic curative resection with extended lymphadenectomy for pancreatic carcinoma. J Am Coll Surg 203:345–352
13. Rea DJ, Heimbach JK, Rosen CB, et al. (2005) Liver transplantation with neoadjuvant chemoradiation is more effective than resection for hilar cholangiocarcinoma. Ann Surg 242:451–458
14. Padhani AR, Liu G, Koh DM, et al. (2009) Diffusion-weighted magnetic resonance imaging as a cancer biomarker: consensus and recommendations. Neoplasia 11:102–125
15. Wang J, Takashima S, Takayama F, et al. (2001) Head and neck lesions: characterization with diffusion-weighted echo-planar MR imaging. Radiology 220:621–630
16. Le Bihan D, Breton E, Lallemand D, et al. (1986) MR imaging of intravoxel incoherent motions: application to diffusion and perfusion in neurologic disorders. Radiology 161:401–407
17. Kwee TC, Takahara T, Luijten PR, Nievelstein RA (2010) ADC measurements of lymph nodes: inter- and intra-observer reproducibility study and an overview of the literature. Eur J Radiol 75:215–220
18. Liu S, Wang H, Guan W, et al. (2015) Preoperative apparent diffusion coefficient value of gastric cancer by diffusion-weighted imaging: correlations with postoperative TNM staging. J Magn Reson Imaging 42:837–843
19. Lee J, Kim SH, Kang TW, Song KD, Choi D, Jang KT (2016) Mass-forming intrahepatic cholangi ocarcinoma: diffusion-weighted imaging as a preoperative prognostic marker. Radiology
20. Fattach HE, Dohan A, Guerrache Y, et al. (2015) Intrahepatic and hilar mass-forming cholangiocarcinoma: qualitative and quantitative evaluation with diffusion-weighted MR imaging. Eur J Radiol 84:1444–1451